On the functional design of the DTU10 MW wind turbine scale model of LIFES50+ project

2016 J. Phys.: Conf. Ser. 753 052018

(http://iopscience.iop.org/1742-6596/753/5/052018)

On the functional design of the DTU10 MW wind turbine scale model of LIFES50+ project

I. Bayati[1*], M. Belloli[1], L. Bernini[1], E. Fiore[1] H.Giberti[2], A.Zasso[1]

[1]Politecnico di Milano, Department of Mechanical Engineering, Milan, Italy
[2]Universita' degli Studi di Pavia, Dip. Ingegneria Industriale e dell'Informazione, Pavia, Italy

E-mail: ilmasandrea.bayati@polimi.it*, marco.belloli@polimi.it, luca.bernini@polimi.it, enrico.fiore@polimi.it, hermes.giberti@unipv.it, alberto.zasso@polimi.it

Abstract. This paper illustrates the mechatronic design of the wind tunnel scale model of the DTU 10MW reference wind turbine, for the LIFES50+ H2020 European project. This model was designed with the final goal of controlling the angle of attack of each blade by means of miniaturized servomotors, for implementing advanced individual pitch control (IPC) laws on a Floating Offshore Wind Turbine (FOWT) 1/75 scale model. Many design constraints were to be respected: among others, the rotor-nacelle overall mass due to aero-elastic scaling, the limited space of the nacelle, where to put three miniaturized servomotors and the main shaft one, with their own inverters/controllers, the slip rings for electrical rotary contacts, the highest stiffness as possible for the nacelle support and the blade-rotor connections, for ensuring the proper kinematic constraint, considering the first flapwise blade natural frequency, the performance of the servomotors to guarantee the wide frequency band due to frequency scale factors, etc. The design and technical solutions are herein presented and discussed, along with an overview of the building and verification process. Also a discussion about the goals achieved and constraints respected for the rigid wind turbine scale model (LIFES50+ deliverable D.3.1) and the further possible improvements for the IPC-aero-elastic scale model, which is being finalized at the time of this paper.

1. Introduction

LIFES50+ is an H2020 EU project, which aims at proving cost effective technology for floating substructures for 10MW wind turbines, at water depths greater than 50 m. The objective is optimizing and qualifying, to a Technology Readiness Level (TRL) of 5, two innovative substructure designs for 10MW wind turbines, as well as developing a streamlined and a key performance indicator KPI based methodology for the evaluation and qualification process of floating substructures. The reference 10 MW wind turbine is the one developed by DTU [1], which is taken as reference for the scale model tests. More specifically, LIFES50+ project implements a novel experimental approach to test floating wind turbines, with the main goal of overcoming the scaling issues, typically associated to a system simultaneously loaded by wind and waves (i.e. Froude/Reynolds conflict) and exploiting separately the advantages of ocean basins and wind tunnel testing facilities. The approach consists in the "Hardware-In-The-Loop" hybrid testing approach where the motion of the scale model being tested is given based on the physical wind or wave forcing and respectively on the real-time computed wave or wind forcing (ocean basin or wind tunnel). The real-time system providing the forces is represented by a

set of fish lines actuated by electrical motors and springs in series (force control) moving the model in the Marintek ocean basin [2] or by a 2 degree-of-freedom (DoF) or 6 DoF robot [3, 4] providing the motion at the base of the tower of the wind turbine model at the Politecnico di Milano. As regards the robot, given the constraints in terms of available space in the wind tunnel and overall payloads acting on the end-effector, it is impossible to use the most diffused serial kinematic manipulators; instead Parallel Kinematic Manipulators (PKM) seems to be the best choice for this specific application ([5]). The main drawback in using PKMs is represented by their reduced workspace with respect to their size; thus an optimization process is necessary to guarantee the desired working volume ([6, 7]). In addition, if machine elements are not properly designed, vibration phenomena may arise, mainly due to the slender structure of the links and to the compliance of transmission units as highlighted in [8]. Some methods to compensate vibration phenomena are reported in [9, 10].

The main objectives of LIFES50+ project are the experimental validation of numerical code for assessing the aerodynamic loads arising on wind turbines(i.e. FAST/AeroDyn), as well as HIL/hybrid tests on aero-elasto-dynamic models in the wind tunnel. That's the reason why two different machine are realized: a rigid one which is suitable for the experimental validation within the first wind tunnel session; an aero-elastic one for the second phase. While for the first turbine there's no need to pay too much attention on the masses of the functional subgroups, the constraints on the matching of the inertial and structural properties for the aero-elastic model are very strict in order to guarantee the similarity conditions imposed by the aerodynamic scaling that will be discussed later. This paper presents the design process of the rigid model, illustrating the design choices related to each functional group. The following sections are organized as follows: Section II presents the technical specifications and the design constraints imposed by the aerodynamic scaling of the reference 10 MW wind turbine; Section III deals with the design and the dimensioning of the elements found in each subgroup; Section IV compares the achieved results and the goals imposed by the scaling laws.

2. Technical Specifications

Consistently with previous experiences at Politecnico di Milano Wind Tunnel in wind turbine scale model design ([11],[12] and [13]) and in order to avoid great wind tunnel blockage ratio and to stretch as much as possible the wind speed working range of the test facility within the turbine operational range, the length and velocity scale factors λ_L and λ_V, were respectively set to 75 and 2, more details can be found also in [15] and [17]. Combining these two scale factors it is easy to get the scale factors of all the physical quantities involved as reported in Table 1. These scale factors allowed to define the structural properties of the components of the model as well as the requirements for the motors and the controllers. Table 2 shows the main parameters of the model. As it can be noticed the constraints regarding the mass are very strict, especially the ones related to the nacelle and the rotor: considering the presence of three motors dedicated to the IPC control, the main shaft motor the slip ring in the nacelle, which represent mandatory components with non modifiable masses, and represent almost the major percentage of the overall mass. Therefore, these requirements are very hard to be met and sometime imposing to test ins slightly different conditions compared to the initial scaling factor targets. Nevertheless the first wind turbine prototype realized for the deliverable 3.1 of the project ([14]) is a rigid model so that the mass constraints were not to be respected compulsory, whereas for the aero-elastic model, which is being finalized by the time of this paper, the correct reproduction of the natural frequencies (e.g. overall tower fore-aft) requires a special attention to overall mass of the rotor and nacelle. However, a good starting point for the final aero-elastic machine design is represented by the rigid model version, which allowed to set up the overall mechatronic design, giving also a useful overview of the non-negligible mass contribution due to minor elements (e.g. screws, glue, cables etc.) and to properly design the modification on the

rigid version of the model, for the aero-elastic one, to reach a wind turbine scale model meeting the requirements in terms of scaled natural frequencies, as closest as possible to the target.

Quantity	Scaling Rules	Values
Length	λ_L	75
Speed	λ_V	2
Rotor speed	$\lambda_\omega = \frac{\lambda_V}{\lambda_L}$	$1:37.5$
Frequency	$\lambda_f = \frac{\lambda_V}{\lambda_L}$	$1:37.5$
Time	$\lambda_T = \frac{\lambda_L}{\lambda_V}$	37.5
Acceleration	$\lambda_{acc} = \lambda_L \lambda_f^2$	$1:18.75$
Force	$\lambda_F = \lambda_V^2 \lambda_L^2$	22500
Mass	$\lambda_M = \lambda_L^3$	1687500

Table 1. Scaling Factors

Parameter	Full Scale	Wind tunnel	Physical Unit
Cut-in speed	4	2	m/s
Rated speed	11.4	5.7	m/s
Cut-out speed	25	12.5	m/s
Minimum rotor speed	6.0	225	rpm
Maximum rotor speed	9.6	360	rpm
Rotor diameter	178.3	2.37	m
Blade length	86.4	1.15	m
Hub high	119	1.58	m
Blade mass	$42 * 10^3$	$9.95 * 10^{-2}$	kg
Nacelle mass	$442 * 10^3$	1.05	kg
Rotor mass	$228 * 10^3$	0.55	kg
Tower mass	$628 * 10^3$	1.49	kg
Ct rated	0.814	0.814	–
Cp rated	0.476	0.476	–
Rated thrust	1619	$7.1 * 10^{-2}$	kN
Rated torque	10738	$6.36 * 10^{-3}$	kNm
Tilt angle	5	5	deg

Table 2. Turbine scaled parameters

3. Design

With regard to Figure 1 three different functional groups can be identified:

- *Nacelle*: the nacelle represents the connection between the tower and the rotor; the characteristic elements of this group are the main shaft motor, which is misaligned with respect to the main shaft. The transmission is realized by means of a toothed belt. It is important to mention the presence of the slip ring which guarantees the connection to the IPC motors, in terms of power supply and digital/analog signals input/ouput.
- *Rotor*: two subgroups can be identified, the hub and the blades. Two different pitch control mechanisms were designed, a manual one, adopted during the first wind tunnel session for the deliverable 3.1 ([14]), and the motor-drive IPC system.

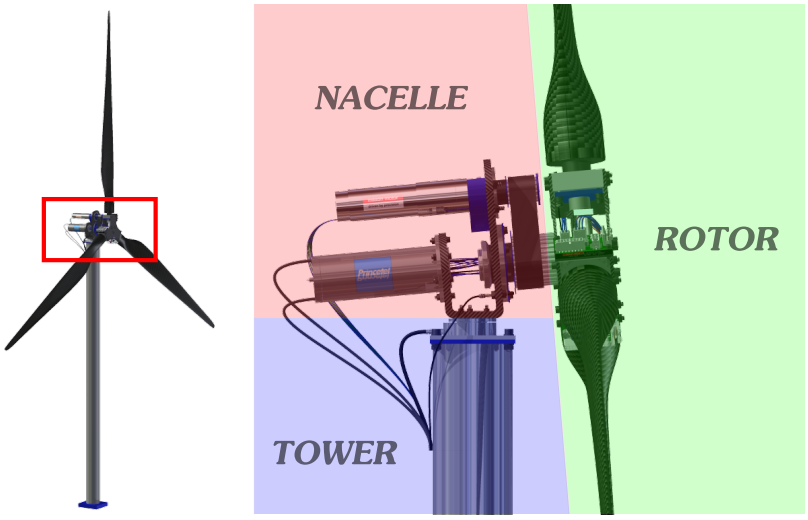

Figure 1. Scale model wind turbine assembly.

- *Tower top*: the functional element of the tower is a 6-axes balance which is placed between the nacelle and a connection flange on the top of the tower to measure the overall rotor forces.

3.1. Nacelle

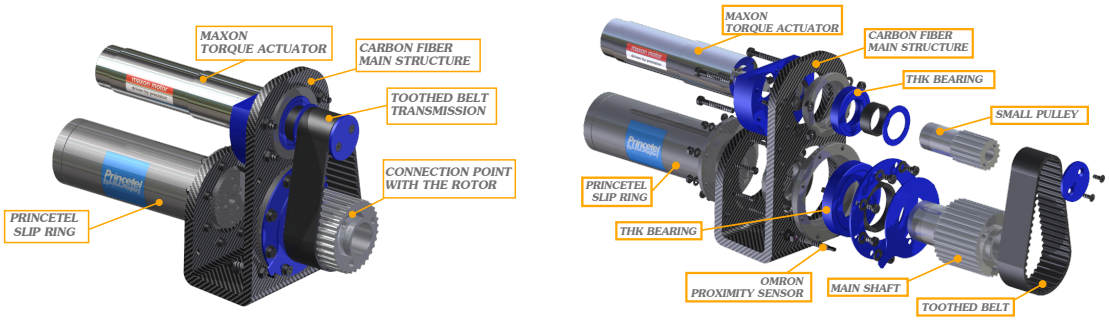

(a) Nacelle assembly. (b) Nacelle exploded view.

Figure 2. Nacelle CAD model.

The nacelle, represented in Figure 2, is characterized by a "U-shaped" structure made of high modulus carbon fiber structure, whose aim is to guarantee the correct positioning of the main shaft motor, the slip ring device, the main shaft and the rotor tilt angle. In addition, the bottom surface of this element is directly connected to the 6-axes balance. The frontal surface is inclined in order to guarantee the prescribed 5° tilt angle for the main shaft, Table 2. The high stiffness of the carbon fiber allows to have a very thin structure and to reduce the overall weight. The reason behind the choice of putting the main shaft and the principal motor on two different axes is to allow the electrical cables coming from the slip ring to reach the drives of the IPC motors, this required also that main shaft is hollowed. Another innovative feature is the system used to support both the main shaft and the pulley to which the principal motor is connected; indeed the usage of classical ball bearing to bear bending moments would require

two of these elements for each axis, leading to a bigger structure and to an increase of weight. Cross-roller bearings seemed to be the best choice, since they allow to save space and to bear very high bending moments with the same weight of a single ball bearing. Two aluminum cases directly glued to the carbon fiber structure are devoted to hold the external cup of the cross-roller bearings. While the upper bearing external cup is glued to the aluminum case, the bottom one is constrained by means of an aluminum flange fixed to the aluminum case by means of a set of screws.

As mentioned, the transmission of the motion from the principal motor to the main shaft is realized by means of a toothed belt that introduces a transmission ratio equal to 2. The idea of using a gear-to-gear coupling has been discarded because it would have led to an excessive increment of mass.

With regard to the dimensioning of the principal motor, and taking into account the specifications illustrated in Table 2, the transmission ratio introduced by the toothed belt, the principal motor was required to have the following characteristics:

$$T_{req} = 3.15\,Nm \qquad \Omega = 720\,rpm \qquad P = 237\,W \tag{1}$$

In general it is not difficult to find a commercial solution that meets these characteristics, but the restrictions on the mass considerably reduced the possible candidates. The best solution turned out to be a brushless DC motor *EC-4 Pole 30* by *Maxon* equipped with a *GP 32 HP* planetary gear with a transmission ratio of $21:1$ and a magnetic encoder with a resolution of $500\,[1/rev]$. The principal motor is fixed to the carbon fiber structure by means of a rigid plastic support element (ABS) realized with a 3D printer.

3.2. Rotor

As mentioned before the rotor can be further divided into the hub and the three blades. A view of the rotor is reported in Figure 3. The structural support of the blades roots is given by two carbon fiber triangular plates and by three aluminum blocks, whose aim is to keep the distance between the two plates, as well as to hold the two versions of the pitch regulation mechanisms. In order to make the hub even stiffer three carbon fiber hollowed spacers are placed between the plates. As can be noticed, the plate which is in contact with the main shaft is characterized by a hole that allows to mount the rotor on the main shaft with a high precision centering between the rotor axis and the main shaft itself. Furthermore this kind of coupling provides the correct transmission of the shear stresses from the rotor to the main shaft and then to the cross-roller bearing. The fixing between hub and main shaft is achieved by means of three long screws that go through the plates and the spacers to end up into three threaded holes located on the frontal surface of the main shaft. For this application it is also mandatory to eliminate the risk of vibration phenomena that would invalidate the results. It is thus of fundamental importance to ensure that the hub structure is sufficiently stiff by performing a Finite Element Method (FEM) analysis to check the correct design. The FEM model shown in Figure 4 takes into account the presence of the aluminum blocks at the three ends of the hub, whose mass cannot be neglected, especially if one considers that the big distance from the axis of rotation leads to an increase of the inertia and consequently to a reduction of the frequency associated to the first mode of vibration of the structure. Fortunately, the carbon fiber employed makes the structure very rigid. A width of $3\,mm$ is sufficient to increase the frequency associated to the first mode of vibration to $68\,Hz$, ensuring a greatly higher frequency compared to the first flap-wise blade natural frequency, approximately of 22 Hz, see [15].

With regard to the design of the connection between the hub and the blades, the cross-roller bearings turned out to be the best choice, also considering the small available space, to bear the estimated loads at the blade's root. The chosen cross-roller bearing is the *RB2008* by *THK*; this is the smallest and lighter cross-roller bearing produced by *THK*, and is capable to bear up to

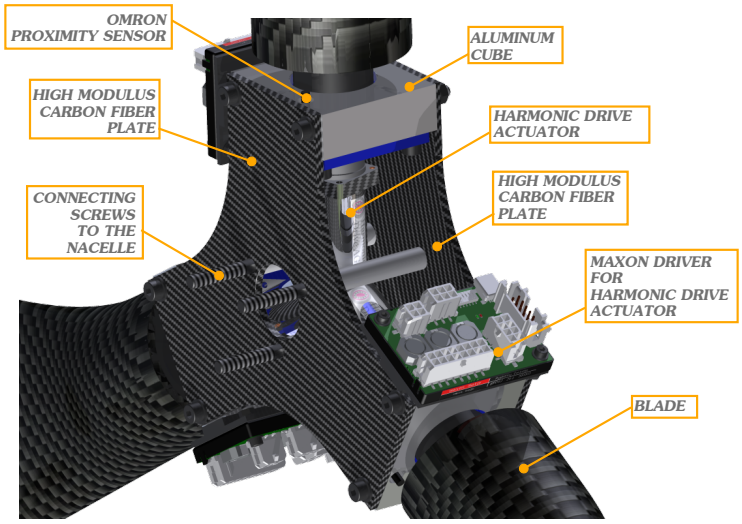

(a) Rotor assembly.

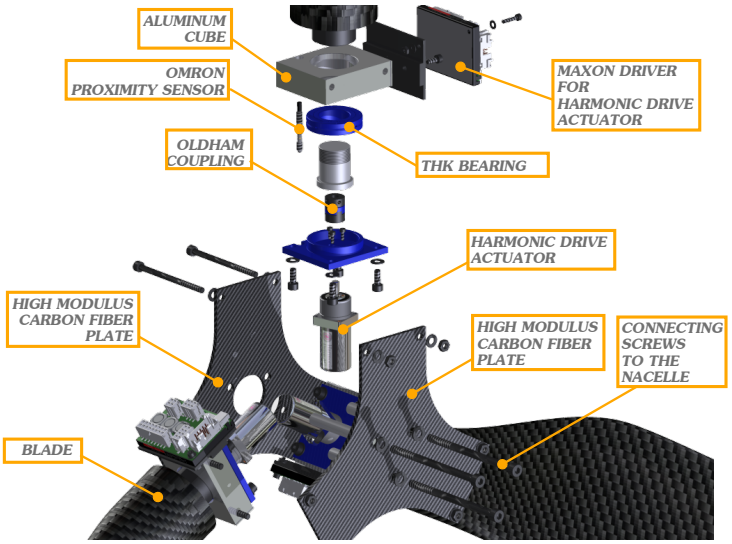

(b) Rotor exploded view.

Figure 3. Rotor CAD model.

40 Nm. The housing for the outer cup is realized within the aluminum blocks, and the blockage is guaranteed by an aluminum flange. Furthermore, an aluminum plug is glued into the blade at the root, in order to have an aluminum element connecting the blade to the hub, whereas on the hub side a small cap hosts the Oldham joint, Figure 3. Between these two components the inner cup of the cross-roller bearing is located. A FEM analysis (ABAQUS®) was carried out with the same goal to verify that these elements had a sufficiently high stiffness not to interfere with the blade frequency. For this specific case, the bearing and the block are assumed to be infinitely rigid, whereas the overall mass and moment of inertia of the blade is modeled as a concentrated element properly coupled. The results of the FEM simulation (Figure 5) show that the first eigen frequency is around 200 Hz, which can be can be considered satisfactory.

Regarding the IPC mechanism, Harmonic Drive motors were chosen since they allow to regulate the pitch of the blades with zero backlash and very high dynamic performances,

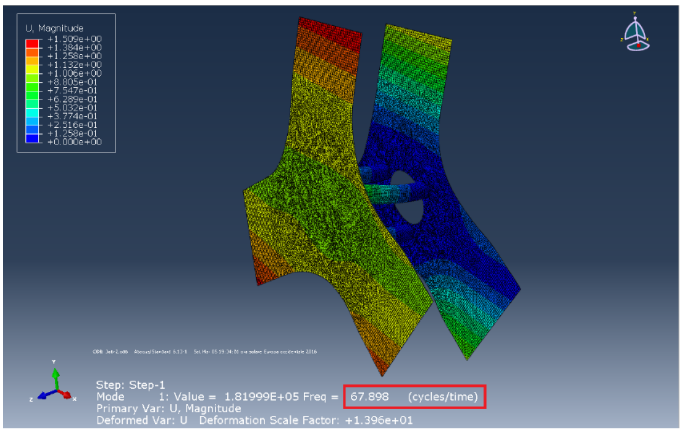

Figure 4. FEM model of the hub.

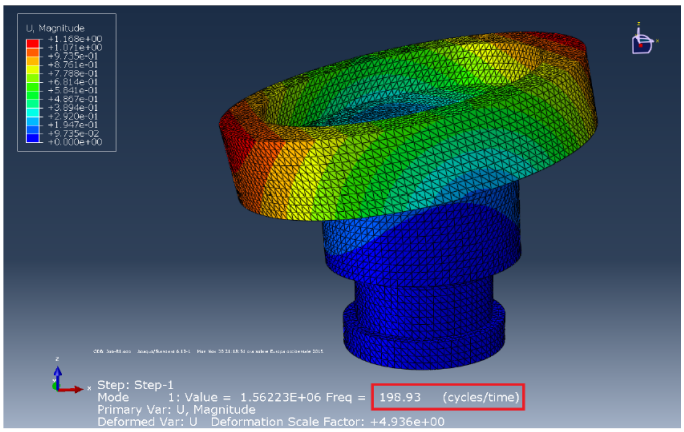

Figure 5. FEM model of the plug.

controlled in position. The choice of the motor was due to the performance 3P target assuming an amplitude $A = 5°$ at nominal angular speed $\Omega_{nom} = 360\,rpm$. The dimensioning rms values of the angular displacement θ, angular speed $\dot{\theta}$, and angular acceleration $\ddot{\theta}$, assume the following values:

$$\theta_{rms} = \frac{A}{\sqrt{2}} = 0.062rad; \quad \dot{\theta}_{rms} = \frac{3 \cdot A \cdot \Omega_{nom}}{\sqrt{2}} = 6.98rad/s; \quad \ddot{\theta}_{rms} = \frac{A \cdot (3 \cdot \Omega_{nom})^2}{\sqrt{2}} = 789.29rad/s^2 \tag{2}$$

The same approach was used to compute peak values associated to these quantities:

$$\theta_{peak} = A = 0.087rad; \quad \dot{\theta}_{peak} = 3 \cdot A \cdot \Omega_{nom} = 9.87rad/s; \quad \ddot{\theta}_{peak} = A \cdot (3 \cdot \Omega_{nom})^2 = 1116.23rad/s^2 \tag{3}$$

With these results the *nominal* and *maximum* torque required to the motors were computed following the procedure described in [16]:

$$T_{rms} = J_{tot}\ddot{\theta}_{rms}; \quad T_{peak} = J_{tot}\ddot{\theta}_{peak}; \tag{4}$$

where J_{tot} represents the overall moment of inertia about the motor axis. This parameter takes into account the contributions given by the blade, the plug, the inner cup of the bearing,

the cap, the Oldham joint, and also the contribution of the reducer. Since the required angular resolution is very small, the Harmonic Drive motors represent the best choice with an almost zero backlash, a high positioning precision and a high transmission ratio. Furthermore, the reducers are lighter with respect to the classic planetary gear. The chosen motor is the *RSF Mini 5B* with a $1:30$ transmission ratio, a $0.9 \cdot 10^{-3} rad$ positioning precision and an inertial moment $J_{gear} = 6.6 \cdot 10^{-5}\, kg \cdot m^2$. With the information related to the actuator it is possible to verify if the chosen motor is able to meet the torque requirements. The overall moment of inertia is estimated to be equal to $J_{tot} = 22.19 \cdot 10^{-5}\, kg \cdot m^2$. The resulting *rms* and *peak* torque value are respectively:

$$T_{rms} = 0.175\, Nm; \quad T_{peak} = 0.248\, Nm; \tag{5}$$

For the motor sizing the aerodynamic torque contribution was neglected for being negligible compared to the inertia contribution for the required amplitude and frequency of motion. The motor under analysis is able to meet these requirements as can be noticed looking at its working range in Figure 6.

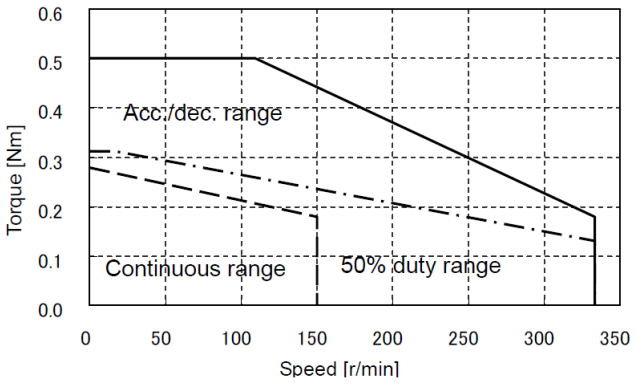

Figure 6. Harmonic Drive working range.

3.3. Tower top

Figure 7 shows the assembled and exploded view of the tower top. The principal element is the 6-axes balance whose top surface is directly connected to the nacelle carbon fiber structure whereas the bottom surface is fixed to an aluminum plate which is fixed to an aluminum plug glued to the tower. The balance is a *Mini 45* by *ATI* which is able to measure forces up to $\pm 145\, N$ along the x and y directions, and up to $\pm 290\, N$ along the z axis. Furthermore, it is able to measure torques up to $\pm 5\, Nm$ about all the axes.

During all the design process a parametric approach has been adopted, especially for the aero-elastic version of the model. The CAD model was linked to an *.xls* containing the mass properties of each component of the assembly, allowing also a direct view of the effect on the overall mass due to any modification and to compare them with the requirements. Table 3 shows the final masses of the functional groups compared to the down-scaled DTU 10MW wind turbine as reported on deliverable 3.2 ([14], under review) of LIFES50+ project.

4. Conclusions

This paper presented the methodological approach, the final design and the features of the wind turbine rigid scale model of the LIFES50+ project. The adopted scaling factors and the consequent strict constraints on the masses are discussed. The functional subgroups are

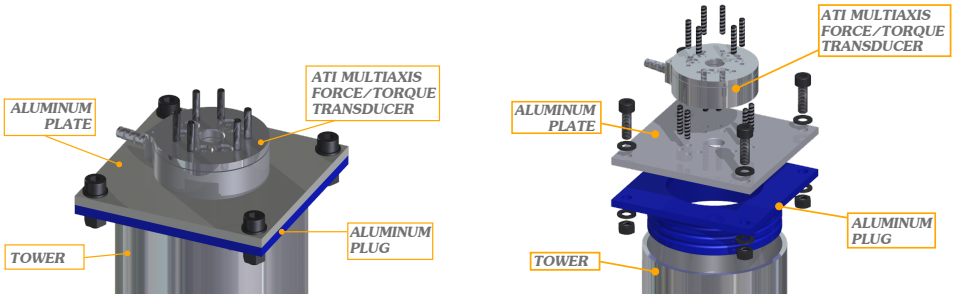

(a) Tower top assembly. (b) Tower top exploded view.

Figure 7. Tower top CAD model.

Assembly	DTU 10MW RTW $[kg]$	DTU down-scaled $[kg]$	PoliMi 10MW WTM $[kg]$
Nacelle	446036	1.057	1.788
Rotor (blade+hub)	227962	0.540	1.255
Single blade	41716	0.099	0.210

Table 3. Mass goals and results.

presented in detail, illustrating the innovative features introduced and the choices leading to the final version of the model. Even if during the first wind tunnel session the first prototype of the wind turbine scaled model was supposed to be rigid and not aero-elastic, a particular attention was reserved to the reduction of the overall mass, even at this stage. The IPC mechanism is designed taking into account the interchangeability with the manual mechanism used during the first phase of tests (i.e. validation of FAST/AeroDyn, [17]). The realized model shown in Figure 8 is considered to have met the functional requirements, as good results have been gathered from the first testing campaign [17]. However, by the time of this document the aero-elastic version of the scale model is being finalized with a special attention to the nacelle overall mass and stiffness constraints.

References

[1] C. Bak et Al, "The DTU 10-MW Reference Wind Turbine",Technical University of Denmark, DTU Wind Energy, Denmark, 2013.
[2] E. Bachynski, V. Chabaud, T. Sauder, "Real-time Hybrid Model Testing of Floating Wind Turbines: Sensitivity to Limited Actuation", Energy Procedia, Volume 80, 2015.
[3] I. Bayati, M. Belloli, A. Facchinetti, and S. Giappino. "Wind tunnel tests on floating offshore wind turbines: A proposal for hardware-in-the- loop approach to validate numerical codes". Wind Engineering, 2012.
[4] Bayati, I., Belloli, M., Ferrari, D., Fossati, F., Giberti, H. "Design of a 6-DoF robotic platform for wind tunnel tests of floating wind turbines (2014) Energy Procedia", 53 (C), pp. 313-323.
[5] Giberti, H., Ferrari, D. A novel hardware-in-the-loop device for floating offshore wind turbines and sailing boats (2015) Mechanism and Machine Theory, 85, pp. 82-105.
[6] Ferrari, D., Giberti, H. "A genetic algorithm approach to the kinematic synthesis of a 6-DoF parallel manipulator" 2014 IEEE Conference on Control Applications, CCA 2014, art. no. 6981355, pp. 222-227.
[7] Fiore, E., Giberti, H. "Optimization and comparison between two 6-DoF parallel kinematic machines for HIL simulations in wind tunnel" (2016) MATEC Web of Conferences, 45, art. no. 04012, .
[8] Fiore, E., Giberti, H., Ferrari, D. "Dynamics modeling and accuracy evaluation of a 6-DoF Hexaslide robot (2016)" Conference Proceedings of the Society for Experimental Mechanics Series, 1, pp. 473-479.
[9] N. Negahbani, H. Giberti, E.Fiore, Error Analysis and Adaptive-Robust Control of a 6-DoF Parallel Robot

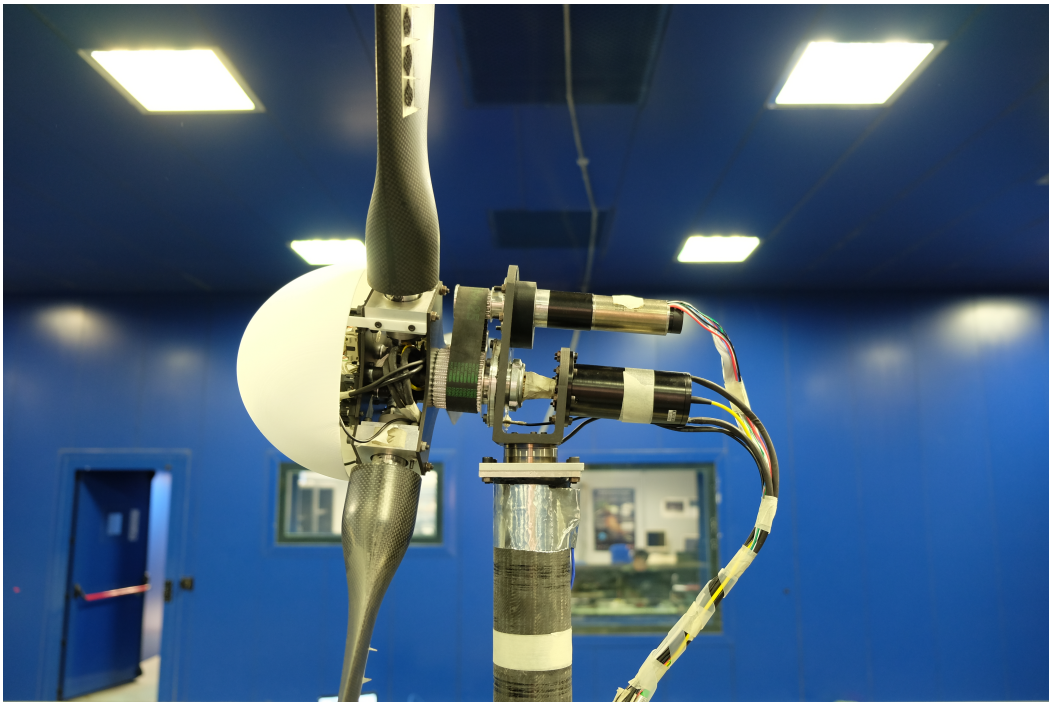

Figure 8. Physical model of the rigid wind turbine.

with Ball-Screw Drive Actuators, Journal of Robotics, vol. 2016, Article ID 4938562, 15 pages, 2016. doi:10.1155/2016/4938562

[10] Giberti, H., Cinquemani, S., Ambrosetti, S. "5R 2dof parallel kinematic manipulator - A multidisciplinary test case in mechatronics" (2013) Mechatronics, 23 (8), pp. 949-959.

[11] H. Bredmose, "Contribution to InnWind Deliverable 4.22, Scaling laws for Floating wind turbine testing". DTU Wind Energy. 2014

[12] C. Bottasso, F. Campagnolo and V. Petrovic. "Wind tunnel testing of scaled wind turbine models: Beyond aerodynamics." Journal of Wind Engineering and Industrial Aerodynamics, 2014

[13] F. Campagnolo, C. Bottasso and P. Bettini "Design, manufacturing and characterization of aero-elastically scaled wind turbine blades for testing active and passive load alleviation techniques within a ABL wind tunnel.", TORQUE, 2014.

[14] H2020 LIFES50+ project: `http://lifes50plus.eu/`

[15] I. Bayati, M. Belloli, L. Bernini, R. Mikkelsen, A. Zasso. "On the aero-elastic design of the DTU 10MW wind turbine blade for the LIFES50+ wind tunnel scale model", Journal of Physics: Conference Series, The Science of Making Torque from Wind, 2016.

[16] Giberti, H., Cinquemani, S., Legnani, G. A practical approach to the selection of the motor-reducer unit in electric drive systems (2011) Mechanics Based Design of Structures and Machines, 39 (3), pp. 303-319.

[17] I. Bayati, M. Belloli, L. Bernini, A. Zasso. "Wind tunnel validation of AeroDyn, within LIFES50+ project: imposed Surge and Pitch tests", Journal of Physics: Conference Series, The Science of Making Torque from Wind, 2016.